

Suspensions of fluor-containing nanoparticles for quantifying β -emitting radionuclides in non-hazardous media

Donghua Zhu, Zhongjiang Mu, Caleb Mooty, Michelle Kovarik, and Michael Jay

Department of Pharmaceutical Sciences, University of Kentucky, Lexington, KY 40536-0082, USA
Corresponding author: Jay, M. (jay@email.uky.edu).

Nanoparticles containing scintillants were prepared from oil-in-water microemulsions in which styrene–divinylbenzene comprised the oil phase. Primary and secondary fluors [2,5-diphenyloxazole and 1,4-bis(2-methylstyryl) benzene] were dissolved in the oil phase, which was emulsified with dodecyl trimethylammonium bromide or sodium dodecyl sulfate before polymerization by the addition of sodium persulfate. The resulting suspension qualified as non-hazardous waste by testing against US EPA standards for reactivity, pH, ignitability, and toxicity characteristic leaching. ^{14}C -glycerol was added to the aqueous nanoparticle suspension and to a conventional organic scintillation cocktail, and the relative efficiency of detection was obtained by liquid scintillation counting. The results were compared with a mathematical model that predicted the effect of particle size and concentration on the probability of an emitted β^- particle interacting with a suspended particle. The use of these nanoparticle suspensions represents an opportunity to reduce mixed low-level radioactive hazardous waste generated by liquid scintillation counting.

Introduction

Liquid scintillation (LS) counting is a routine, but effective tool for measuring the concentration of radioisotopes in samples obtained during pharmaceutical research. The mechanism behind LS involves the mixing of a radiolabeled analyte with a liquid medium that is capable of transferring the kinetic energy of nuclear emissions into solvent molecules with subsequent transfer to, and excitation of,

detector (fluor) molecules. The de-excitation of the fluors results in the emission of light, which is subsequently quantified by photomultiplier tubes in an LS counter [1,2].

The primary solvents used to solubilize the aromatic fluors are usually non-polar and aromatic, but many of the samples containing β^- -emitting radionuclides that pharmaceutical and biomedical researchers are interested in analyzing are aqueous in nature. Initial approaches during the

1950s to quantify the amount of radioactivity in aqueous samples containing ^{14}C -labeled compounds involved the addition of fluor-containing fibers or solids (e.g., Pilot B: a polyvinyltoluene bead containing *p*-terphenyl and diphenylstilbene) to the aqueous samples. The poor contact between the β^- emitter and the fluors owing to the short range of the emitted β^- particles resulted in low detection efficiencies. Later, emulsion-based LS 'cocktails' composed of organic solvents, fluors, and surfactants were developed in which aqueous radioactive samples could be emulsified before being counted in an LS counter. This remains the basic technology used to quantify radioactivity in aqueous samples by LS counting [3-6]. Although advances have been made in the development of biodegradable cocktails, the disposal of scintillation cocktail waste, some of which continues to comprise 'mixed' (radioactive and organic) waste, remains an environmental and economic issue.

We began to explore the possibility of using an aqueous formulation for quantifying α - and β -emitting radionuclides. Our work in drug development involving poorly water-soluble compounds demonstrated that their apparent solubility could be enhanced up to 10 000-fold by entrapping them in the oil droplets of an oil-in-water microemulsion, which served as a precursor to engineered nanoparticles [7]. We subsequently described a 'NanoScintillation System', which is an aqueous suspension of fluor-containing polystyrene nanoparticles for quantifying β^- emitters by LS counting. To prepare these nanoparticles, an oil-in-water microemulsion was created with the aid of surfactants in which fluors were dissolved in the oil (styrene) droplets. Subsequent polymerization of the styrene phase produced polystyrene nanoparticles that contained entrapped fluors [8]*†. The surfactants used to form the microemulsion align at the interface between the nanoparticle and the aqueous medium, providing surface-charge repulsion, which keeps these nanoparticles in a suspended state. The efficiency of energy transfer from the emitted β^- particle to the fluors in this suspension depends on the particle energy, the distance it must travel in the medium before interacting with a nanoparticle, and the nature of the medium. Given that water does not have the energy-transfer character of the organic solvents used in commercial LS cocktails, a decrease in counting efficiency is expected when quantifying low-energy β^- emitters in this system, owing to the energy loss when β^- particles travel through water.

The current work describes our efforts to enhance the detection efficiency of the NanoScintillation System for low-energy β^- emitters by producing suspensions of smaller nanoparticles with higher particle concentrations. This is expected to decrease the distance between the β^- emitter and the fluor-containing nanoparticles. The effects of styrene concentration, choice of surfactant, and surfactant:monomer ratio on particle size and particle concentration of the system were evaluated. Theoretical calculations

based on the Fermi distribution, mean free path, and stopping power equations also were used to predict the relationship between the counting efficiency and particle size and concentration of the nanoparticle suspensions.

Experimental methods

Preparation of NanoScintillation System

All reagents were purchased from Sigma (St Louis, MO; <http://www.sigma.com>) except sodium dodecylsulfate (SDS), which was obtained from Spectrum Chemical (Gardena, CA; <http://www.spectrumchemical.com>). Styrene was distilled under reduced pressure before use.

Oil-in-water microemulsions were prepared using styrene and divinylbenzene (DVB) as the oil phase, either dodecyltrimethylammonium bromide (DTAB) or SDS as the surfactant, and 1-pentanol as the co-surfactant. PPO (2,5-diphenyloxazole) and bis-MSB [1,4-bis(2-methylstyryl)benzene] as primary and secondary fluors were dissolved in the styrene-DVB phase before the addition of the surfactant solution. Polymerization of the styrene phase was achieved by the addition of sodium persulfate (SPS).

Either SDS or DTAB were dissolved in DI water and stirred continuously upon addition of 0.2% (v/v) 1-pentanol. Freshly distilled styrene solutions were purged with N_2 for 20 min. PPO (3.45 mg ml^{-1}) and bis-MSB (0.27 mg ml^{-1}) were dissolved in a styrene-DVB (DVB = 3.65 mg ml^{-1}) mixture in an ultrasonic bath. The aqueous surfactant solution was then added, forming a microemulsion; this was followed by the addition of SPS (0.2 mg ml^{-1}) and subsequent heating at 70°C for 8 h. This polymerization step resulted in the formation of an aqueous suspension of fluor-containing polystyrene nanoparticles. To study the effect of styrene concentration on particle size, mixtures of 60, 45, and 30 mg ml^{-1} of styrene with 100 mg ml^{-1} SDS or DTAB were used to make microemulsions SDS-1, 2, 3 and DTAB-1, 2, 3, respectively. To study the effect of the surfactant:monomer ratio on particle size, preparations containing 60 mg ml^{-1} styrene with a 0.314:2 surfactant:monomer ratio were used to make microemulsions SDS-4, 5, 6 and DTAB-4, 5.

The particle size of the resulting nanosuspensions was measured by photon correlation spectroscopy using a Coulter N4 Plus Submicron Particle Sizer (Coulter, Miami, FL; <http://www.beckman.com>) by scattering light at 90° at 25°C for 90 s. A fixed amount of ^{14}C -glycerol (15 000 disintegrations min^{-1} ; DPM) was added to each suspension (1 ml), which were subsequently placed in an LS counter (Beckman Multi-Purpose Scintillation Counter, LS 6500) without automatic quench correction. The same amount of ^{14}C -glycerol was added to a conventional organic LS cocktail (Fisher Scintiverse BD; <http://www.fishersci.com>), which also was placed in an LS counter. The number of counts per minute (CPM) obtained from the LS counter was acquired for all samples ($n = 3$; samples counted to an error of 1%) and re-

Continued on page 78.

ported as relative counting efficiency (CPM of nanosuspension/CPM of conventional organic cocktail). The background of the nanoparticles when no ¹⁴C was added was ~30 CPM and is similar to that obtained for the LS cocktail.

Testing for disposal as non-hazardous waste

Samples of the NanoScintillation Systems were sent to an independent analytical and environmental testing laboratory (TestAmerica, Inc., Nashville, TN; http://www.testamericainc.com) to determine whether it qualified as non-hazardous as per Subparts C and D of 40 CFR Part 261. These included tests for toxicity characteristic leaching procedure (TCLP) extraction by US EPA 1311, TCLP for volatile organic compounds by US EPA Method 1311/8260B, TCLP for semi-volatile organic compounds by US EPA Method 1311/8270C, TCLP for metals by 6000/7000 series methods, and tests for reactivity, pH, and ignitability.

The theoretical model

A model was developed to describe the relationship between detection efficiency and the size and concentration of the nanoparticles. A computational code based on the energy spectrum of emitted β⁻ particles and the energy loss as these particles travel through a medium was processed using MATLAB 7.0. The first step in this model was to mimic the energy spectrum of ¹⁴C, which can be computed from the Fermi distribution [9] (Equation 1):

$$N(E) = K(E^2 + 2Em_0c^2)^{1/2}(Q - E)^2(E + m_0c^2)F(Z, E) \quad (\text{Eqn 1})$$

where $N(E)$ is the number of β⁻ particles in the energy range between E and $E + dE$; Q is the maximum energy of a β⁻ particle; K is a normalizing constant; m_0c^2 is the rest mass energy of an electron; and $F(Z, E)$ is the Fermi function (Equation 2):

$$F(Z, E) = 2\pi n/[1 - \exp(-2\pi n)] \quad (\text{Eqn 2})$$

where n is defined as Ze^2/hv (Z = atomic number of the daughter isotope, h is the reduced Plank constant, and v is the velocity of the electron). In this case, 1560 particles from 0 to 0.156 Mev with an interval 0.0001 Mev were used to simulate the energy spectrum of ¹⁴C.

The second step was to determine the length of the path that the β⁻ particle needs to travel before encountering a fluor-containing nanoparticle. Because water molecules do not exhibit the energy-transferring capacity observed with organic solvents used in LS cocktails, the energy lost by the β⁻ particle depends largely on the distance it must travel through the medium, as well as on the stopping power of the medium. Because the initial velocity of the β⁻ particle is much larger than the movement of nanoparticles in the suspension, we can neglect the velocity of the nanoparticles and use the modified mean free path equation to calculate the distance that a β⁻ particle must travel before encountering a fluor-containing nanoparticle [10] (Equation 3):

$$\text{Mean free path} = 1/(10^4 \pi r^2 C) \quad (\text{Eqn 3})$$

Batches	Styrene (mg ml ⁻¹)	S:M ratio ^a	Particle size (nm) ^b	Particle density (no. ml ⁻¹)	MFP (nm) ^c	RCE ^d	
SDS	1	60	1.67	37 (0.8)	2.15E+15	432	0.339
	2	45	2.22	33.1 (0.8)	1.71E+15	514	0.258
	3	30	3.33	27.4 (0.9)	2.65E+15	639	0.153
	4	60	2	30.4 (0.9)	3.88E+15	354	0.385
	5	60	0.628	48.5 (1.5)	9.57E+14	566	0.238
	6	60	0.314	69.2 (2.4)	3.29E+14	807	0.140
DTAB	1	60	1.67	34.8 (1.2)	2.59E+15	406	0.319
	2	45	2.22	30.6 (0.5)	2.86E+15	476	0.307
	3	30	3.33	23.2 (1.7)	4.37E+15	514	0.224
	4	60	1.5	104.5 (4.1)	9.56E+13	1219	0.184
	5	60	1.33	221 (5.2)	1.16E+13	2462	0.143

^aSurfactant:monomer (styrene) weight ratio. ^bMean values +/-sd, (n = 3). ^cMFP, mean free path.
^dRelative counting efficiency for ¹⁴C of SDS and DTAB nanoparticle preparations in which the surfactant used was either SDS or DTAB.

*Weekley, J.C. *et al.* (2002) Nanosuspensions as aqueous scintillation cocktails. 16th Annual Meeting of American Association of Pharmaceutical Scientists, 10-14 November 2002, Toronto, Canada

†Weekley, J.C. *et al.* (2002) NanoScintillation systems for aqueous-based liquid scintillation counting. 48th Annual Radiobioassay and Radiochemical Measurements Conference, 11-15 November 2002, Knoxville, TN, USA

Table 1. Suspensions of fluor-containing nanoparticles.

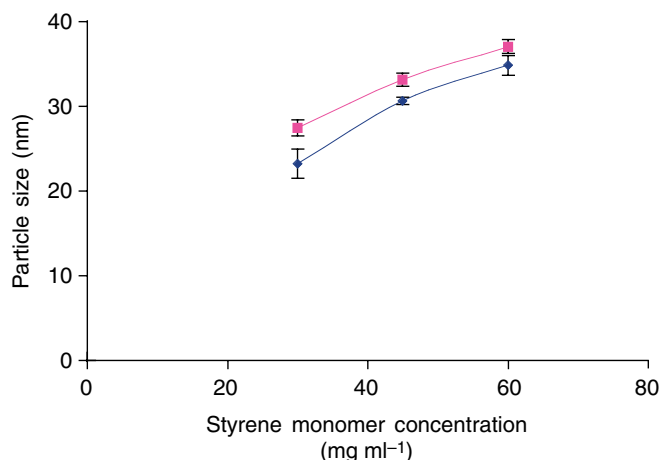


Figure 1. Particle size of fluor-containing nanoparticles as a function of the styrene concentration used in the preparation of microemulsions with SDS (solid squares) or DTAB (solid diamonds) as the surfactant (100 mg ml⁻¹) before polymerization with 0.2 mg ml⁻¹ SPS ($n = 3$). As the concentration of styrene was increased, the ratio of free radicals (formed from the thermal decomposition of SPS) to the monomer decreased. This was expected to result in a higher degree of chain propagation and larger particle size.

(measured in cm), where r is the mean radius of the nanoparticles (m) and C is the concentration of the nanoparticles (no. ml⁻¹), which can be determined by Equation 4:

$$C = \frac{3M}{(10^6 4\pi r^3 \rho)} \quad (\text{Eqn 4})$$

(measured as no. ml⁻¹), where M is the styrene mass concentration (g ml⁻¹) and ρ is density of polystyrene (g ml⁻¹), assuming all the initial styrene monomer will be polymerized and form particles, and that the weight of the particle can be determined by the mass of polystyrene. Substituting Equation 3 into Equation 4 gives a simple expression for mean free path (Equation 5):

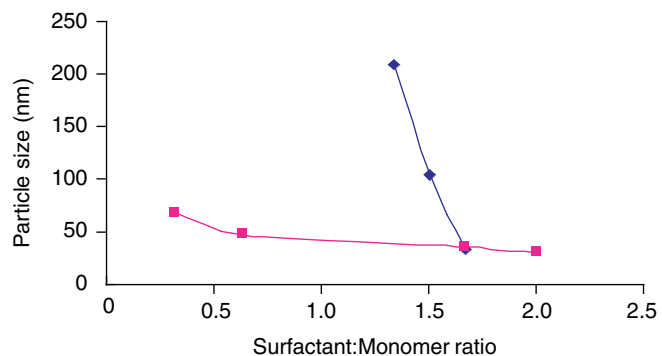


Figure 2. Particle size as a function of the surfactant:monomer ratio (w/w) used in the preparation of microemulsions with SDS (solid squares) or DTAB (solid diamonds) as the surfactant before polymerization with SPS (0.2 mg ml⁻¹). Styrene concentration was held at 60 mg ml⁻¹ ($n = 3$). Surfactant is required to reduce the interfacial tension, which results in a negative free energy change and a decrease in particle size.

$$\text{Mean free path} = \frac{400rp}{3M} \quad (\text{Eqn 5})$$

(measured in cm). The loss of energy by charged particles traveling through a material is divided into two components based on the mechanism of energy transfer (either collision or radiative energy loss), which can be calculated by the total stopping power (Equation 6):

$$\frac{dE}{dx} = (dE/dx)_{\text{col}} + (dE/dx)_{\text{rad}} \quad (\text{Eqn 6})$$

(measured in Mev cm⁻¹), where $(dE/dx)_{\text{col}}$ is the electronic energy loss owing to Coulomb interactions (i.e., ionization and excitation), and $(dE/dx)_{\text{rad}}$ is the nuclear energy loss (e.g., owing to emission of Bremsstrahlung or Cerenkov radiation, and nuclear interactions). Because the kinetic energy of ¹⁴C is low, $(dE/dx)_{\text{col}} / (dE/dx)_{\text{rad}} > 700$, we used $(dE/dx)_{\text{col}}$ (Mev cm⁻¹) to calculate the energy of the β^- particle absorbed by the medium and/or nanoparticles (Equation 7):

$$\frac{dE}{dx} = \frac{2\pi q^4 NZ}{m_e v^2} \left[\text{In} \left(\frac{m_e v^2 E}{2I^2(1-\beta^2)} \right) - (2\sqrt{1-\beta^2} - 1 + \beta^2) \text{In}(2) + (1 + \beta^2) + \frac{(1 - \sqrt{1 - \beta^2})^2}{8} \right] \quad (\text{Eqn 7}) [11],$$

where z is atomic number of the ionizing particle ($z = 1$ for β^- particles); q is a unit electrical charge (1.6×10^{-19} C); m_e is the rest mass of an electron (9.1085×10^{-28} g); v is the velocity of the ionizing particle; N is the number of absorber atoms cm⁻³; Z is the atomic number of the absorber; NZ is the number of electrons cm⁻³ in the absorber; β is the fraction of the speed of light particle is traveling (v/c); c is the speed of light in a vacuum (3×10^8 m s⁻¹); and I is the mean excitation and ionization potential for water (79.7 ± 0.5 eV) [12].

Once the absorption of β^- particle energy by water molecules was calculated, it was assumed that conversion of energy to emitted light, the detection of photons, and the signal amplification by a scintillation counter were the same as those for a conventional organic LS cocktail. Thus, the calculated counting efficiency also was reported in relative values equivalent to Energy(remaining)/Energy(initial).

Results and discussion

To improve the detection efficiency (number of CPM measured) of the nanosuspension, the composition of the system was varied in terms of styrene monomer concentration, choice of surfactants, and the surfactant:monomer weight ratio. The resultant nanoparticle suspensions were translucent and homogeneous, and can be stored at room temperature without an increase in size over time. The data for all prepared batches are listed in Table 1.

Continued on page 80.

Monomer concentration

As shown in Figure 1, there is a direct relationship between the concentration of styrene used to prepare the microemulsion precursor and particle size. For this experiment, the concentration of SPS and surfactant were kept constant at 0.2 mg ml⁻¹ and 100 mg ml⁻¹, respectively. Once SPS was dissolved in water and heated, it decomposes to form radical units. A relatively constant number of radical units are expected to be produced for all of the SDS and DTAB batches. As the concentration of styrene was increased, the ratio of free radicals (formed from the thermal decomposition of SPS) to the monomer decreased. This was expected to result in a higher degree of chain propagation; larger particles were produced, similar to the results reported elsewhere [13-15]. However, although a lower styrene monomer concentration might yield a smaller mean particle radius (from the numerator of Equation 5), the styrene monomer concentration in the denominator of Equation 5 indicates that a simple decrease in styrene concentration might not necessarily result in an increase in detection efficiency.

Surfactant effects

The radical anions formed by the thermal decomposition of SPS might be influenced by the surface charge of the microemulsion droplets. When using the cationic surfactant DTAB to form the microemulsion, an electrostatic attraction with the radical anion might result in an increase of the overall flux of radicals entering the microemulsion droplets. This could lead to a larger number of initiation and termination events, and would be expected to produce shorter polymer chains, resulting in a smaller particle size after polymerization of the microemulsion droplet is complete. The opposite holds when using the anionic SDS as the surfactant. Figure 1 shows that nanoparticles prepared with SDS as the surfactant are larger than those prepared with DTAB as the surfactant.

The function of the surfactant and co-surfactant in the microemulsions is to reduce the interfacial tension γ_{12} between the oil and water phases and can be described by Equation 8:

$$\Delta G_{form} = \Delta A\gamma_{12} - T\Delta S_{conf} \quad (\text{Eqn 8})$$

where ΔA is the change in interfacial area A (equal to $4\pi r^2$ per droplet of radius r); ΔG_{form} is the free energy for creating new interfacial area; T is temperature (Kelvin); and ΔS_{conf} is the configurational entropy change. Small droplets with their high number densities yield an increase in total surface area ΔA and a positive ΔS_{conf} value. Surfactant is required to reduce the interfacial tension, which results in a negative free energy change. As shown in Figure 2, as the surfactant:monomer ratio increases, the size of the resulting par-

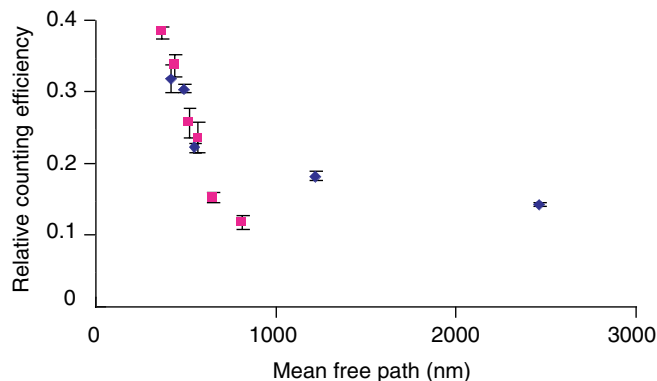


Figure 3. Relative counting efficiency (CPM of NanoScintillation System/CPM of scintillation cocktail) measured in a liquid scintillation counter ($n = 3$) as a function of the calculated mean free path (DTAB, solid diamonds; SDS, solid squares). The shorter the distance that the β^- particle travels through the water, the less energy it will lose and the more likely it is to encounter a fluor-containing nanoparticle and be detected.

ticles decreases. However, at low surfactant:monomer ratios, the particle size of batches prepared with DTAB as the surfactant increases. This is not observed for batches prepared with SDS as the surfactant and might be due to the differences in the critical micellar concentrations of DTAB (~16 mM) compared with SDS (~1 mM). At lower surfactant:monomer ratios, there is not a sufficient amount of DTAB to support a microemulsion structure. Small droplet sizes in the microemulsion, which yield small particles following polymerization of the styrene-DVB droplets, can be obtained using a high styrene concentration and the addition of larger quantities of surfactant to account for an increase in surface area. Similar results have been reported

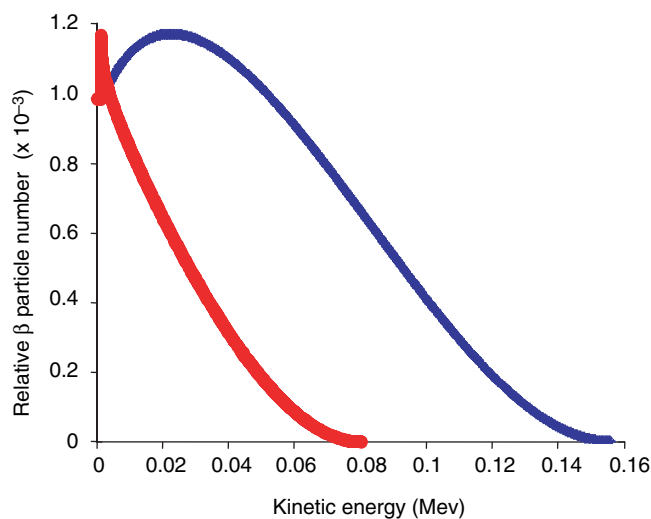


Figure 4. Simulated energy spectra of ¹⁴C for an ideal, unquenched sample (blue line) and the NanoScintillation System (red line). The quenched spectrum is due to absorption of β^- energy by the water molecules in the nanosuspension.

elsewhere [16]. Nanoparticle suspensions prepared in such a way have shorter mean free paths and higher relative counting efficiencies (Figure 3).

The use of greater surfactant concentrations could have disadvantages, such as signal attenuation and/or quenching and yielding a product with a greater percent of solids in the disposal of the nanosuspension. The overall effect of the composition of the system on the detection efficiency of various α - and β -emitting radionuclides, and how the composition affects waste disposal issues, are currently under investigation. One approach to avoiding higher surfactant concentrations would be to use high shear to reduce the microemulsion droplet size before polymerization.

Non-hazardous waste testing

Testing of NanoScintillation System samples to determine

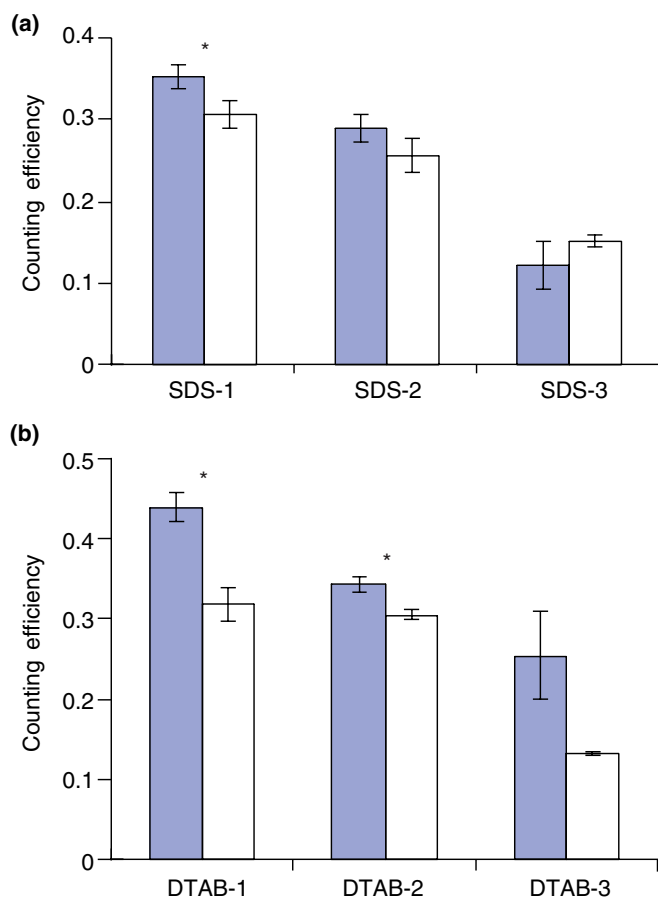


Figure 5. Comparison of the calculated (solid bars) counting efficiency with experimentally determined (open bars) relative counting efficiency ($n = 3$) for NanoScintillation Systems SDS 1–3 (a) and DTAB 1–3 (b). * indicates a statistically significant difference ($p < 0.05$) using a t -test. The statistical difference between the theoretical model and the observed results for DTAB-batches and SDS-1 produced from higher styrene concentrations might be due to the fact that the theoretical model does not take into account the chemical quenching effect of the surfactant molecules or other factors, such as optical quenching.

whether they qualified as non-hazardous as per Subparts C and D of 40 CFR Part 261 demonstrated that the flash point of the suspension was $>200^{\circ}\text{F}$ and that the pH was 7.4 with no detectable reactive cyanide or sulfide. No metals, volatile or semi-volatile organic compounds were detectable using US EPA methods.

Mean free path

The distance that an emitted β^- particle must travel before encountering a fluor-containing nanoparticle, which depends on particle size and initial styrene concentration in the microemulsion, can be determined by calculating its mean free path. The shorter the distance that the β^- particle travels through the water, the less energy it will lose and the more likely it will be to encounter a fluor-containing nanoparticle and be detected. Figure 3 shows the effect of the mean free path on the relative counting efficiency; the slope is directly related to the stopping power dE/dx (Mev cm^{-1}). As expected, the relative counting efficiency decreases with an increase in mean free path; the stopping power is constant in the mean free path range of 300–600 nm.

Theoretical model

The theoretical unquenched ^{14}C energy spectrum and the quenched spectrum owing to absorption of β^- energy in the nanosuspension were simulated using the model described earlier and are depicted in Figure 4. Experimentally obtained data indicated that suspensions of smaller nanoparticles and higher particle concentrations (which result in a shorter mean

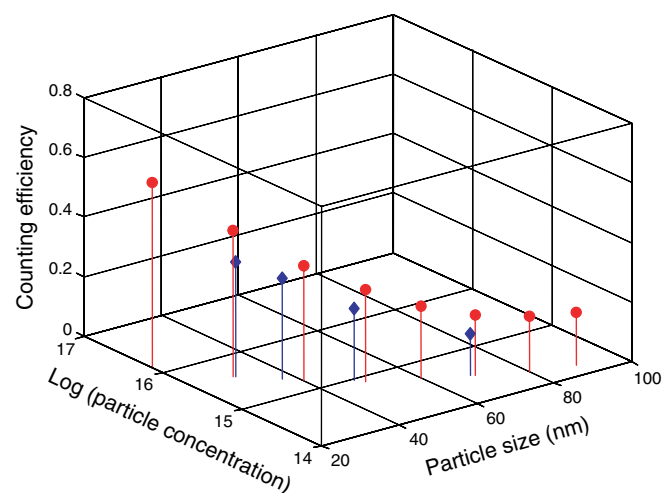


Figure 6. Relationship between particle size, particle concentration and calculated (solid circles) counting efficiency and experimentally determined (solid diamonds) relative counting efficiency of the NanoScintillation Systems (SDS batches 1, 4, 5, and 6). The experimental results indicated that a higher concentration of smaller particles could reduce the mean free path of emitted β^- particles and improve the detection efficiency of the NanoScintillation System, as predicted by theoretical calculations.

Continued on page 80.

free path of emitted β^- particles) yield higher relative counting efficiencies, as predicted by the theoretical model. A comparison of the counting efficiency of the SDS and DTAB nanoparticle batches calculated by the model with the experimentally determined relative counting efficiency is shown in Figure 5. The theoretical results agree with the experimentally obtained data ($p > 0.05$) when lower amounts of styrene are used in the preparation of the microemulsion precursor (SDS-2 and SDS-3) and the resulting suspension has a lower concentration of nanoparticles.

The statistical difference ($p < 0.05$) between the theoretical model and the observed results for DTAB-batches and SDS-1 produced from higher styrene concentrations might be due to the fact that the theoretical model does not take into account the chemical quenching effect of the surfactant molecules, or other factors, such as optical quenching. So that it can be used to design a suspension with an optimum concentration of particles for maximum detection of β^- particles, the theoretical model is being refined to account for these effects, which might result from higher particle concentrations. The model should be easily adapted for other β^- emitters of different maximum energies.

Figure 6 shows the relationship between particle size, particle concentration and relative counting efficiency for both calculated and experimentally observed results with the SDS batches. The current model predicts that, if the size of the nanoparticles could be reduced to 20 nm, the counting efficiency could be improved to 62% for ^{14}C using batches prepared with an initial styrene concentration of 60 mg ml^{-1} .

Conclusion

NanoScintillation Systems comprising fluor-containing polystyrene particles were prepared from oil-in-water microemulsions with subsequent polymerization of the oil phase (styrene-divinylbenzene). The size of the particles, as well as their concentration, is dependent upon the starting concentration of the monomer (styrene), the type of surfactant, and the surfactant:monomer ratio. Larger particles are produced when using large initial amounts of styrene, resulting in low surfactant:monomer ratios, and when there is an electrostatic repulsion between surfactant molecules and generated free radicals. The distance that a β^- particle emitted from a ^{14}C nucleus must travel in the medium before interacting with a suspended nanoparticle (mean free path) can be calculated because it is proportional to particle size and inversely proportional to monomer concentration.

The experimental results indicated that a higher concentration of smaller particles could reduce the mean free path of emitted β^- particles and improve the detection efficiency of the NanoScintillation System, as predicted by theoretical calculations. The theoretical model can be used to design an optimum concentration of particles for optimum detection of β^- particles over a wide energy range, but needs

to be refined to account for quenching effects. The aqueous suspensions of fluor-containing nanoparticles qualified as non-hazardous waste using US EPA test methods.

These results demonstrate that the NanoScintillation System, which does not use organic solvents, can be used in place of conventional scintillation cocktails when high sensitivity is not required. The lower detection efficiency for ^{14}C is offset by the expected savings in the cost of waste disposal. Initial studies with other radionuclides indicate that the detection efficiency of the NanoScintillation System might be equivalent to conventional scintillation cocktails for higher-energy β^- emitters.

Acknowledgements

The authors gratefully acknowledge financial support from the National Science Foundation Grant DMR-0097692 and the Kentucky Science and Education Foundation Grant KSEF-563-RDE-005 as well as helpful comments from Marcus McEllistrem, Professor Emeritus of Physics, University of Kentucky.

References

1. Kessler, M.J. (1989) *Liquid Scintillation Analysis, Science and Technology*, Packard Instrument Co.
2. Steinberg, D. (1958) Radioassay of carbon-14 in aqueous solutions using a liquid scintillation spectrometer. *Nature* 182, 740-741.
3. Myers, L.S. and Brush, A.H. (1962) Counting of alpha and beta radiation in aqueous solutions by the detergent-anthracene scintillation method. *Anal. Chem.* 34, 342-345.
4. Harrah, L.A. and Powell, R.C. (1971) Dose rate saturation in plastic scintillators. In *Organic Scintillators and Liquid Scintillation Counting* (Horrocks D.L. and Peng C.T., eds), pp 265-278, Academic Press.
5. Schram, E. (1970) Flow-monitoring of aqueous solutions containing weak β^- emitters. In *The Current Status of Liquid Scintillation Counting* (Bransome, E.D., ed.), pp 95-109, Grune & Stratton.
6. Ewer, M.J.C. and Harding, N.G.L. (1974) Micellar scintillators: a rational approach to the design of stable assay solvents for liquid scintillation counting. In *Liquid Scintillation Counting* (vol. 3) (Crook, M.A. and Johnson, P., eds), pp 220-233, Heyden & Son.
7. Oyewumi, M.O. *et al.* (2004) Comparison of cell uptake, biodistribution and tumor retention of folate-coated and PEG-coated gadolinium nanoparticles in tumor-bearing mice. *J. Cont. Rel.* 95, 613-626.
8. Weekley J.C. *et al.* (2004) Aqueous liquid scintillation counting with fluor-containing nanosuspensions. *Appl. Rad. Isotop.* 60, 887-891.
9. Wakabayashi, G. *et al.* (2003) Evaluation of the self-absorption of ^{14}C beta-rays in gel-suspension samples by Monte Carlo simulation. *J. Radioanalyt. Nuc. Chem.* 255, 585-590.
10. IUPAC (1997) *IUPAC Compendium of Chemical Terminology* (2nd edn), IUPAC.
11. Leroy, C. and Rancoita, P.G., eds (2004) *Principles of Radiation Interaction in Matter and Detection*, World Scientific Publish Co.
12. Dingfelder, M. *et al.* (1998) Electron inelastic-scattering cross sections in liquid water. *Rad. Phys. Chem.* 53, 1-18.
13. Westbrook, J.A. *et al.* (2001) Microemulsion polymerization: an undergraduate experiment in the synthesis of nanosized polystyrene particles. *Chem. Educator* 6, 104-108.
14. Wang, L.M. *et al.* (1998) Synthesis and evaluation of a surface-active photoinitiator for microemulsion polymerization. *Macromolecules* 31, 3446-3453.
15. Guo, J.S. *et al.* (1989) Microemulsion polymerization of styrene. *Polym. Sci. A* 27, 691-710.
16. Landfester, K. *et al.* (1999) Formulation and stability mechanisms of polymerizable miniemulsions. *Macromolecules* 32, 5222-5228.